Uniform Circular Array Pattern Synthesis Using Second-Order Cone Programming

W. Mark Dorsey, Jeffrey O. Coleman, *Senior Member, IEEE*, and William R. Pickles

***Abstract*—Here we formulate second-order cone programs (SOCPs) for synthesizing complex weights for far-field directional (single-point mainbeam) patterns for narrowband arrays. These formulations, while constructed here with the uniform circular array (UCA) in mind, are actually quite general in that they control the arbitrary-pol sidelobe level (SLL) and co-pol SNR loss relative to ideal by minimizing either while upper-bounding the other. The SLL can be addressed in either an L-infinity sense or an L1 sense, and elements are assumed characterized by individual embedded complex patterns, modeled or measured, and so need not be identical. Conformal arrays are the obvious application, but we leave that for others and here instead apply the SOCPs to uniform circular arrays of directional elements. Design examples assume an antipodal Vivaldi element design with an embedded element pattern obtained through simulation using appropriate unit-cell boundary conditions. Rotation and translation of that simulated pattern provides embedded element patterns for all elements of the circular array.**

***Index Terms*—Antenna phased arrays, Optimisation, Beamforming arrays**

I. Introduction

A uniform circular array (UCA) offers full coverage of the azimuth plane with either a more-or-less omnidirectional radiation pattern or with electronically steerable directional beams. The directional beams can be electronically scanned in the azimuth plane without significant changes to the beamwidth and sidelobe level (SLL)[1], [2].

Pattern synthesis and beam steering are more challenging for a UCA than for traditional linear and planar arrays because the UCA steering vectors do not have a Vandermonde structure. Subsequently, common UCA beamforming techniques discussed in the literature create a virtual array with beam steering vector that is approximately Vandermonde in nature. One common technique uses phase-mode transformations. The work in [3]–[6] has shown these phase-mode transformations can be extended to UCAs of directional elements with benefits to array performance. This technique relies on approximations, however, and degraded performance results in the usual application, direction-of-arrival (DOA) estimation[7]–[9].

If SLL control is required, conventional SLL tapering can be applied to the excitations obtained from the phase-mode transformation. This is done in [10], [11] where a Dolph-Chebyshev approach upper bounds the sidelobe level (SLL) globally. However, the authors in [10] mention that this technique is not guaranteed to maximize the gain of the pattern for a given SLL, and thus more efficient solutions are possible. In [6], an optimization technique upper bounds the SLL of the UCA. However, no constraints are present on array signal to noise ratio (SNR). Moreover, the application of traditional SLL tapers restricts these techniques from synthesizing patterns requiring multiple (or asymmetrical) SLL regions.

This paper take an entirely different approach, one based on an earlier formulation of a second-order cone program (SOCP) to synthesize narrowband patterns from the wavelength scaled array architecture [12]. That work superimposed measured element-level planar near-field (PNF) responses using a vector of complex weights that serve as optimization variables. The weight vector is optimized to minimize array taper loss subject to desired constraints on SLL. That work represented an extension of work done in [13]–[15] that allowed nonidentical embedded element patterns while applying SLL constraints to arbitrarily-polarized signals.

Here, we extend that prior work in yet another direction – this time, by formulating SOCPs suitable for pattern synthesis of a UCA. The geometry of a UCA results in all array elements having unique unique elements patterns because of their unique pointing directions. This formulation accommodates unique embedded element patterns by translating and rotating a unit cell simulation performed in ANSYS HFSS using appropriate boundary conditions. The algorithm presented in [16] formulates SOCPs with similar element-pattern representations for a conformal array – a generalization of the UCA geometry focused on in this paper. However, they synthesized broadened main beams, an inherently nonconvex problem. They solve their nonconvex problem iteratively by using an SOCP to solve a linearized subproblem on each iteration.

In this work we formulate a second-order cone program (SOCP) to synthesize the far-field pattern of the circular array with appropriate signal to noise ratio (SNR) and sidelobe constraints. The ultimate goal here is to integrate polarization constraints in a technique analagous to that in [12] synthesizing a directional pattern for a UCA with optimal SNR and custom SLL constraints. We then optimize the performance of the circular array by solving the SOCP using an NRL-developed front end [17] to a widely available numerical solver. The combination of maximizing SNR with the flexibility of SLL constraint definition gives this pattern synthesis approach advantages over other techniques seen in the literature.

Manuscript received February 3, 2015. This work was supported by the Offie of Naval Research.

W.M. Dorsey and W.R. Pickles are currently with the Radar Division, U.S. Naval Research Laboratory, Washington, DC 20375, e-mail: wmdorsey@vt.edu. J.O. Coleman is retired from the Radar Division.

II. Array Optimization Using SOCPs

Like a linear program, an SOCP specifies optimization of real optimization variables to minimize a real objective function linear in the optimization variables subject to linear equality constraints and linear inequality constraints. In addition, however, an SOCP can include second-order cone constraints. Linear inequality constraints and linear equality constraints take respective forms $a \leq b$ and $y = z$ with real quantities a and b and complex quantities y and z each affine—linear plus a constant—in the optimization variables. A second-order cone constraint takes the form $\|\mathbf{z}\| \leq r$ for some complex vector $\mathbf{z}$ and real scalar r with $\mathbf{z}$ and r affine in the optimization variables.

SOCPs have been used for optimizing linear and planar arrays. However, to the best of the authors' knowledge, they have not been applied to UCAs. Here, we briefly discuss the history of using SOCPs in traditional array pattern synthesis before showing their application to UCAs.

A. Why Convex Programming

Only convex-programming design of element weights is considered here. For narrow beams, convex-program weight/beam designs are easily formulated to constrain or optimize transmit total-power efficiency or receive SNR performance subject to constraints on sidelobe levels in even vast numbers of individual directions. The benefits of convex optimization are that a local optimum is always a global optimum, multiple numerical solvers and usable interfaces to them are readily available, and these solvers are stunningly efficient, easily accomodating designs of hundreds to thousands of weights subject to thousands or tens of thousands of inequality constraints, at least if one can afford—on today's ordinary personal computers—tens of seconds to tens of minutes of optimization time.

B. History of Convex Optimization for Arrays

Serious convex optimization for the design of phased array weights really began with the seminal 1997 paper of Lebret and Boyd [18], which used a custom interior-point algorithm to synthesize a pattern for an array of omnidirectional elements at arbitrary positions on a line. Their formulation, while not identified as such, was actually an SOCP, a type of convex program largely introduced to the application world in a deservedly classic 1998 paper by Lobo, Vandenberghe, Boyd, and Lebret [19]. That paper presented many example SOCPs, both as abstract problems and in specific application contexts. Its somewhat idiosyncratic narrowband receive-array example, however, featured omni elements at arbitrary positions in a plane containing the far-field transmitter, and while the possibility of constraining noise power was mentioned parenthetically, the formulation as presented dealt only with the peak sidelobe level. Uniform line arrays are of course just spatial FIR filters and so were implicitly covered in their FIR-filter discussion, which again addressed only uniform sidelobe bounds.

The earlier work on convex formulations above came from the control-theory and optimization communities, however, and was relatively unsophisticated from an antenna-design point of view, in particular ignoring power efficiency. The iterated-SOCP work cited above came from the DSP community and had the same limitation. Antenna-relevant error measures for SOCP design of planar-array patterns have since been well developed, however. The basic case of constrained minimization of SNR loss in a narrowband receive array of identical elements [20] has been adapted to overlapped subarrays [15] and to an array of nonidentical and nonuniformly placed elements characterized by planar near-field measurements [12]. For wideband digital arrays FIR filters in the elements' individual processing channels can be jointly optimized to create a desired pattern as a function of frequency [13], [21], even with strict control of pattern polarization when dual-pol elements are used [14].

The more recent papers above present design examples computed using widely available SOCP-capable solvers like SeDuMi [22], [23], LOQO [24]–[27], and SDPT3 [28]–[30]. Several high-level optimization languages make these systems relatively easy to use. The optimization community largely works with AMPL [31], a commercial system, while the signal-processing and optimal-control research communities generally favor the available-for-free (in one version, anyway) CVX [32], [33]. Here in the NRL Radar Division we use our own Opt toolbox [34]. While both CVX and Opt layer data types and optimization tools over a Matlab [35] framework, we favor Opt because many of its extras are oriented towards digital-filter and array-antenna problems in particular.

More recently, more involved array problems that are inherently nonconvex have sometimes been addressed with iterative approaches in which each iteration uses an SOCP to solve a convex subproblem. One such problem is the design of the cascade of spatial filters equivalent to a planar-array system structured using overlapped subarrays [36]. Cascades are inherently nonconvex. Another such problem is the shaping of pattern magnitudes across wide main beams while leaving the pattern phase free in the optimization [16]. The required lower bounds on complex magnitudes are inherently nonconvex.

C. Formulating the SOCPs for Array Optimization

The array pattern for an array of N elements

$$\vec{F}(\mathbf{k}) = \sum_{n=1}^{N} w_n \vec{f}_n(\mathbf{k})$$

is defined in terms of the complex excitations $\{w_n\}$ and complex embedded element patterns $\{\vec{f}_n(\mathbf{k})\}$ as discussed in [37]. For a receive array, $\vec{f}_n(\mathbf{k})$ is a receive pattern that is a function of $\mathbf{k}$, which here is the negative of the wavenumber vector for an incident signal. In this paper, we show two SOCP formulations for synthesizing narrowband directional patterns from a phased array. The first method maximizes SNR while upper bounding SLL, and the second method lower bounds SNR while minimizing peak SLL.

1) Optimization with L_∞ SLL Bounds: The simplest way to derive SNR loss is as the degradation in the SNR relative to the best obtainable with any choice of weights. This derivation is adapted from one we presented in [12].

The signal output of the array is proportional to $\mathbf{w}^H\mathbf{f}_{\text{mb}} = \langle \mathbf{f}_{\text{mb}}, \mathbf{w}\rangle$, where $\mathbf{f}_{\text{mb}} = [\vec{f}_n(\mathbf{k}_{\text{mb}}) \cdot \hat{c}]$, where $\hat{c}$ is a unit vector defining co-polarization, where $\mathbf{w} = [w_n]$ is a column vector of complex excitations, where $\mathbf{k}_{\text{mb}}$ is in the direction of the main beam, and where the superscript H denotes the Hermitian transpose. We assume that all elements have identical, individual LNAs and that these LNAs determine the level of circular complex noise contributed to the element output. This noise power is therefore proportional to $\sum_n |w_n|^2 = \|\mathbf{w}\|^2$.

We can introduce a convenient scaling by including a proportionality constant of $\|\mathbf{f}_{\text{mb}}\|^2$ and defining a relative signal-to-noise ratio as the right side of

$$\frac{1}{\Lambda^2} = \frac{|\langle \mathbf{f}_{\text{mb}}, \mathbf{w}\rangle|^2}{\|\mathbf{w}\|^2\|\mathbf{f}_{\text{mb}}\|^2}. \tag{1}$$

We can minimize SNR loss by minimizing the variable Λ introduced on the left while separately forcing equality of the numerators and denominators in (1). The convenience of the scaling in (1) arises from the Schwartz inequality, which upper bounds this relative SNR by unity. Setting $\mathbf{w} = \mathbf{f}_{\text{mb}}$ and substituting $\langle \mathbf{f}_{\text{mb}}, \mathbf{f}_{\text{mb}}\rangle = \|\mathbf{f}_{\text{mb}}\|^2$ in the above shows that the bound can in fact be met with equality, making this a measure of SNR relative to the best achievable. We obtain denominator equality using second-order cone constraint

$$\|\mathbf{w}\|\|\mathbf{f}_{\text{mb}}\| \le \Lambda. \tag{2}$$

Using Λ in no other constraint while making it the objective to be minimized will make (2) hold with equality and so will indirectly minimize $\|\mathbf{w}\|$ subject to the other constraints.

Of course given only this constraint, the optimal $\mathbf{w}$ is the trivial solution with $\mathbf{w} = 0$ and $\Lambda = 0$. To prevent this solution collapse, include the constraint

$$\text{Re}\langle \mathbf{f}_{\text{mb}}, \mathbf{w}\rangle \ge 1.$$

If care is taken to formulate the optimization so that $\mathbf{w}$ can be replaced with $\mathbf{w}\,\mathrm{e}^{j\zeta}$ for any rotation angle ζ without causing either side of any other constraint to change, then the optimization will be free to rotate the elements of $\mathbf{w}$ together in the complex plane in the process of making $\|\mathbf{w}\|$ as small as possible. This process results in $\langle \mathbf{f}_{\text{mb}}, \mathbf{w}\rangle = 1$ and therefore equates the numerators in (2).

To effectively bound the SLL by upper bound δ regardless of polarization, this formulation also includes far-field constraints

$$\sqrt{|\vec{F}(\mathbf{k}_s) \cdot \hat{c}|^2 + |\vec{F}(\mathbf{k}_s) \cdot \hat{x}|^2} \le \delta \tag{3}$$

for $\mathbf{k}_s$ values representing many closely spaced sidelobe directions. Here, complex unit vectors $\hat{c}$ and $\hat{x}$ are (implicitly) functions of $\mathbf{k}_s$ that define co- and cross-polarization respectively. We assume that $\hat{c}$ and $\hat{x}$ are orthogonal and that $\vec{F}(\mathbf{k}_s)$ contains no component normal to them, allowing (3) to be written as $\|\vec{F}(\mathbf{k}_s)\| \le \delta$.

The following SOCP combines the above features.

$$\begin{aligned} &\textit{Optimize} \text{ real variable } \Lambda \text{ and complex vector } \mathbf{w} \\ &\textit{to minimize } \Lambda \\ &\quad \textit{subject to} \text{ noise constraint } \|\mathbf{w}\|\|\mathbf{f}_{\text{mb}}\| \le \Lambda, \\ &\qquad \text{mainbeam constraint } \text{Re}\langle \mathbf{f}_{\text{mb}}, \mathbf{w}\rangle \ge 1, \\ &\qquad \textit{and} \text{ point bounds } \|\vec{F}(\mathbf{k}_s)\| \le \delta \\ &\qquad\quad \text{for } s = 1, 2, \ldots, s_{\max} \end{aligned} \tag{4}$$

The SOCP from (4) can be modified to minimize the peak SLL for a given SNR.

$$\begin{aligned} &\textit{Optimize} \text{ real variable } \delta \text{ and complex vector } \mathbf{w} \\ &\textit{to minimize } \delta \\ &\quad \textit{subject to} \text{ noise constraint } \|\mathbf{w}\|\|\mathbf{f}_{\text{mb}}\| \le \Lambda_0, \\ &\qquad \text{mainbeam constraint } \text{Re}\langle \mathbf{f}_{\text{mb}}, \mathbf{w}\rangle \ge 1, \\ &\qquad \textit{and} \text{ point bounds } \|\vec{F}(\mathbf{k}_s)\| \le \delta \\ &\qquad\quad \text{for } s = 1, 2, \ldots, s_{\max} \end{aligned} \tag{5}$$

While $\|\vec{F}(\mathbf{k}_s)\|$ is shown bounded at individual sidelobe points by a common value value δ, the designer is free to replace δ with fixed bound δ_0 in some proper subset of point bounds if fixed bounds are preferred at some SLL points.

2) Optimization with L_1 SLL Bounds: In Sec. II-C1, we developed SOCPs (4) and (5) containing L_∞ SLL constraints. Here, we modify those formulations to use approximate L_1 SLL constraints instead. The first approach minimizes the SNR loss (Λ) and gives each SLL bound its own variable δ_s. The resulting SOCP

$$\begin{aligned} &\textit{Optimize} \text{ real variable } \Lambda, \text{ complex vector } \mathbf{w}, \\ &\qquad \textit{and} \text{ real variables } \delta_1, \ldots, \delta_{s_{\max}} \\ &\textit{to minimize } \Lambda \\ &\quad \textit{subject to} \text{ noise constraint } \|\mathbf{w}\|\|\mathbf{f}_{\text{mb}}\| \le \Lambda, \\ &\qquad \text{mainbeam constraint } \text{Re}\langle \mathbf{f}_{\text{mb}}, \mathbf{w}\rangle \ge 1, \\ &\qquad \text{point bounds } \|\vec{F}(\mathbf{k}_s)\| \le \delta_s, \\ &\qquad\quad \text{for } s = 1, 2, \ldots, s_{\max} \\ &\qquad \textit{and } \delta_1 + \cdots + \delta_{s_{\max}} \le \delta_0 \end{aligned} \tag{6}$$

then pushes the sum of δ_s below a constant δ_0. Once the minimization forces the constraints to hold with equality, that sum is proportional to a Riemann-sum approximation of $\|\vec{F}(\mathbf{k})\|_1 = \int |\vec{F}(\mathbf{k})|\, d\mathbf{k}$ with the integral taken over the sidelobe region. (This approximate L_1 approach has been used in FIR filter optimization as well [38].)

Alternatively, we can fix the SNR loss to a constant value Λ_0, and minimize the appropriate L_1 sidelobe norm.

$$\begin{aligned} &\textit{Optimize} \text{ real variables } \delta_1, \ldots, \delta_{s_{\max}} \\ &\qquad \textit{and} \text{ complex vector } \mathbf{w} \\ &\textit{to minimize } \delta_1 + \cdots + \delta_{s_{\max}} \\ &\quad \textit{subject to} \text{ noise constraint } \|\mathbf{w}\|\|\mathbf{f}_{\text{mb}}\| \le \Lambda_0, \\ &\qquad \text{mainbeam constraint } \text{Re}\langle \mathbf{f}_{\text{mb}}, \mathbf{w}\rangle \ge 1, \\ &\qquad \textit{and} \text{ point bounds } \|\vec{F}(\mathbf{k}_s)\| \le \delta_s \\ &\qquad\quad \text{for } s = 1, 2, \ldots, s_{\max} \end{aligned} \tag{7}$$

III. Application to a UCA

Consecutive elements numbered $1, \ldots, N$ represent a UCA of N elements if and only if each embedded element pattern

is related to the pattern of element N, taken here to be a sort of prototype, via

$$\vec{f}_n(\mathbf{k}) = \mathbf{R}^n \vec{f}_N(\mathbf{R}^{-n}\mathbf{k}) \tag{8}$$

for some fixed 3×3 rotation matrix $\mathbf{R}$ of index N. By the latter we mean that a full $360°$ of rotation requires N such rotations: $\mathbf{R}^M = \mathbf{I}$ if and only if M is a multiple of N.

Computationally, prototype pattern $\vec{f}_N(\mathbf{k})$ might well itself be constructed by shifting some pattern $\vec{f}_{\text{origin}}(\mathbf{k})$ of an element at the origin out to position $\mathbf{x}_N$ on the array circle:

$$\vec{f}_N(\mathbf{k}) = \vec{f}_{\text{origin}}(\mathbf{k})\, \mathrm{e}^{j\mathbf{k}\cdot\mathbf{x}_N} .$$

As an example, we consider a UCA of Vivaldi radiators having radius of $R = 27.94$ cm (11.0 in.) and operating at 4.0 GHz. The number of elements is varied to explore the impact of the inter-element spacing on the synthesized patterns. The element is modeled in HFSS in a wedge-shaped unit cell with periodic boundaries placed on opposing edges to represent an infinite circular extension as shown in Fig. 1(a). These periodic boundaries are separated by an angle of $2\pi/N$.

The x-y plane of this unit cell is shown in Fig. 1(b) to illustrate the boundaries. The unit cell has four radiation boundaries. Two of these are identified in Fig. 1(b): one is located behind the element at $x = 15$ cm, and another is located at $R_{\text{rad}} = 38$ cm. The other two radiation boundaries are located at the top and botton of the wedge-shaped unit cell at the $\pm\hat{z}$ extents of the computational domain.

The embedded element pattern $\vec{f}_N(\mathbf{k})$ of (8) is obtained from these simulations. For a constant UCA radius, the effective area of the antenna element decreases as the number of elements increases. This changes the gain and beamwidth of the embedded element pattern. These changes are seen in Fig. 2, where we plot the embedded element pattern for the UCA configuration described in Fig. 1 with element counts of 20, 40, 60, and 70. These embedded element patterns are obtained from HFSS simulations. The results show that significant differences are present in the embedded element pattern as the element count changes, and thus the embedded element pattern must precisely reflect the array geometry to synthesize accurate patterns.

Synthesized patterns are shown in Fig. 3(a) for three separate SOCP formulations. Each plot presents results for UCAs with element counts of 20, 40, 60, and 70. In Fig. 3(a), we see results obtained using SOCP (4) to minimize the SNR loss in the array. The results for the case of 20 elements show high SLL and an overall pattern structure that appears largely unusable. When the number of elements is increased to 40, the close-in sidelobes are lowered, but a large lobe is apparent at $\phi = \pm 90°$. Increasing to $N = 60$ eliminates that lobe, and further increasing to $N = 70$ decreases the backlobe significantly.

Fig. 3(b) and Fig. 3(c) show the paterns obtained using SOCPs (5) and (7) to minimize L_∞ and L_1 sidelobes respectively. For these optimizations, the SNR loss was bounded by $\Lambda_0 = 1.5$ dB, and SLL constraints cover the angular region $|\phi| \geq 8°$. Here, we see that the SLL decreases as the number of elements in the array increases. It should be noted that

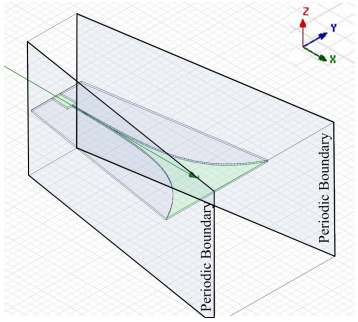

(a) Unit cell for model ($N = 20$)

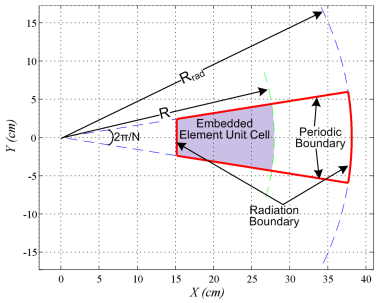

(b) XY plane of the unit cell ($N = 20$)

Fig. 1. HFSS embedded element model for a flared notch elements in a UCA of radius $R = 27.94$ cm operating at 4.0 GHz.

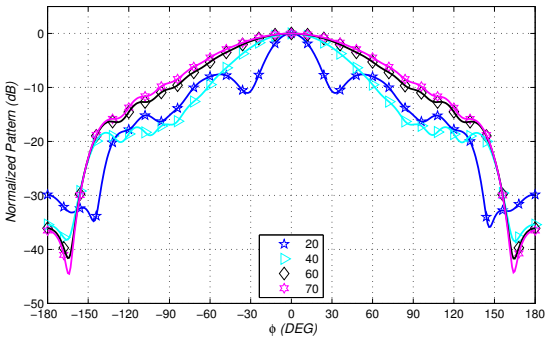

Fig. 2. Embedded element pattern for a single Vivaldi flared notch element in a UCA with 27.94 cm radius with varying number of elements

beamformer implementation must be taken into account to determine practical limits on achievable SLL.

The pattern in Fig. 4 was synthesized for a 70 element array of radius $R = 27.94$ cm at 4.0 GHz using SOCP (4). Here, we have placed SLL constraints asymmetrically about the main beam. The sidelobes for $\phi > 0$ have an upper bound of -30 dB relative to the main beam peak, while the sidelobes for $\phi < 0$ have an upper bound of -40 dB. In addition, two regions of deeply suppresed SLL (i.e. a null region) are located for $-75° \leq \phi \leq -65°$ and $40° \leq \phi \leq 50°$. The sidelobes in these regions have an upper bound of -60 dB relative to the main beam peak. This pattern also used the taper loss constraint defined in (1) which resulted in the optimal design having a taper loss $20\log_{10}\Lambda = 0.563$ dB. This synthesis used a total of 966 constraints and was completed in 0.7 seconds on a typical laptop computer. The pattern synthesis used complex embedded element patterns obtained from HFSS simulations

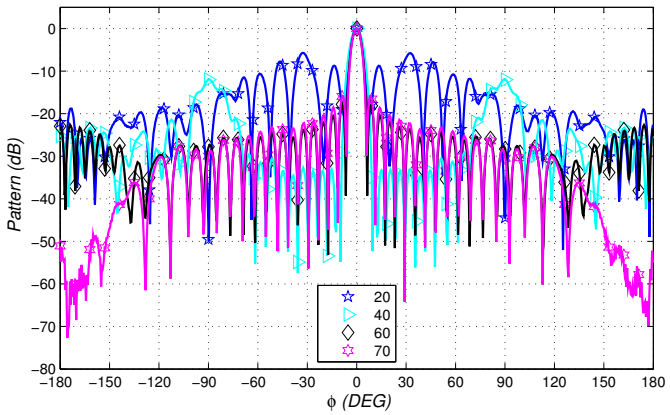

(a) SNR Loss minimization

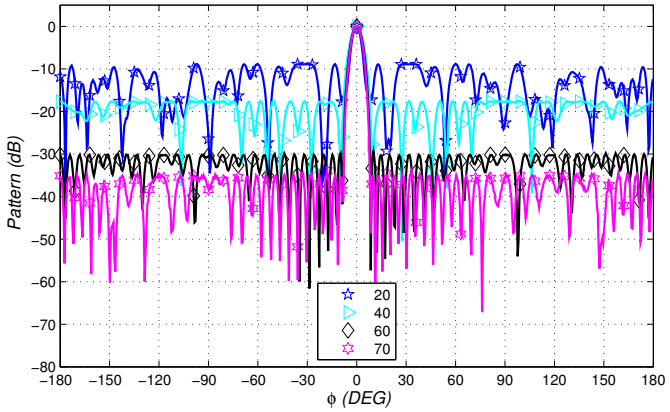

(b) L_∞ SLL minimization ($\Lambda = 1.5$ dB)

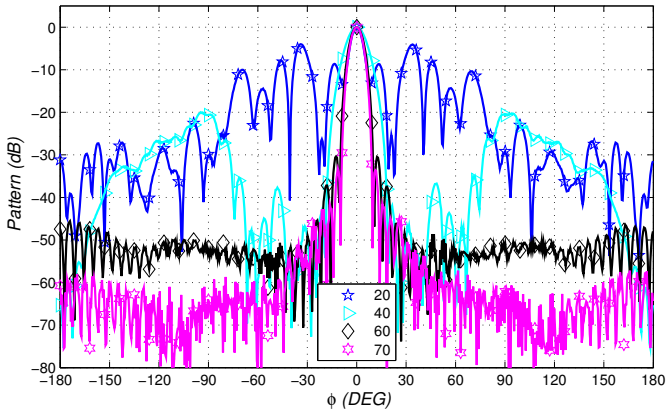

(c) L_1 SLL minimization ($\Lambda = 1.5$ dB)

Fig. 3. Synthesized UCA patterns with SLL minimization formulation with varying number of elements for an array of radius $R = 27.94$ cm at 4.0 GHz.

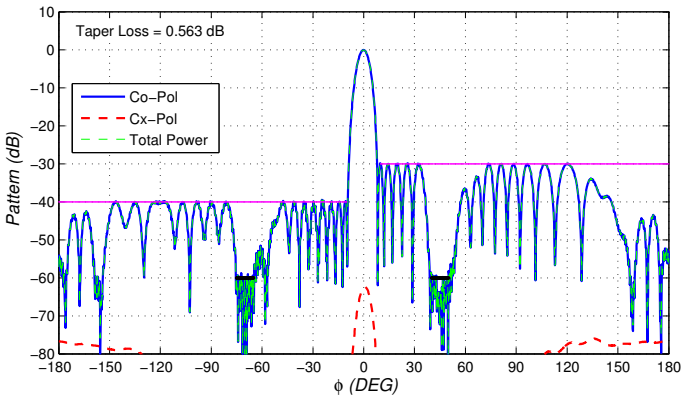

Fig. 4. Synthesized UCA pattern for a 70 element array of radius $r = 27.94$ cm at 4.0 GHz. Asymetrical SLL constraints (-30 dB for $\phi > 0$ and -40dB for $\phi < 0$) were used in conjunction with two null regions that were asymmetrically placed about the main beam region. The location of the SLL and null constraints are shown in magenta and black respectively.

(shown in Fig. 2) and bounded total array pattern obtained using co- and cross-polarized patterns.

IV. Conclusion

This work has shown that second order cone programs (SOCPs) can be formulated to synthesize directional radiation patterns for uniform circular arrays (UCAs). This pattern synthesis technique controls arbitrary sidelobe level (SLL) and co-pol signal-to-noise ratio loss relative to ideal by minimizing either while upper bounding the other. This work demonstrates formulating SOCPs to minimize L_∞ and L_1 sidelobes. It is a straightwoard extension to adapt this formulation to synthesize deeply suppresed null regions in the pattern as shown in the example calculations. The combination of multiple SLL constraint definitions, ability to enforce complex/asymmetrical SLL constraints, and taper loss minimization are benefits of this technique compared to other pattern synthesis techniques for UCAs. The numerical results presented here are consistent with the expectation that increasing the element count while maintaining a constant radius permits lower sidelobes in the optimized pattern for a UCA.

References

[1] J.-A. Tsai and B. Woerner, "Performance of diversity combining for uniform circular arrays," in *Vehicular Technology Conference, 2001. VTC 2001 Fall. IEEE VTS 54th*, vol. 3, 2001, pp. 1630–1634 vol.3.

[2] Q. Shen, E. ke Mao, and W. Si-liang, "The performance analysis of circular array antennas in vhf/uhf band," in *Radar, 2006. CIE '06. International Conference on*, 2006, pp. 1–4.

[3] T. Rahim and D. E. N. Davies, "Effect of directional elements on the directional response of circular antenna arrays," *Microwaves, Optics and Antennas, IEE Proceedings H*, vol. 129, no. 1, pp. 18–22, 1982.

[4] M. Askari and M. Karimi, "Sector beamforming with uniform circular array antennas using phase mode transformation," in *IEEE Iranian Conf. on Electrical Engineering (ICEE)*, 2013, pp. 1–6.

[5] H. Steyskal, "Digital beamforming aspects of wideband circular arrays," in *IEEE Aerospace Conference*, March 2008, pp. 1–6.

[6] F. Belfiori, S. Monni, W. Van Rossum, and P. Hoogeboom, "Side-lobe suppression techniques for a uniform circular array," in *European Radar Conference (EuRAD)*, Sept 2010, pp. 113–116.

[7] M. Askari, M. Karimi, and Z. Atbaee, "Robust beamforming in circular arrays using phase-mode transformation," *IET Signal Processing*, vol. 7, no. 8, pp. 693–703, October 2013.

[8] F. Belloni and V. Koivunen, "Beamspace transform for uca: Error analysis and bias reduction," *IEEE Trans. On Signal Processing*, vol. 54, no. 8, pp. 3078–3089, Aug 2006.

[9] B. K. Lau, Y. H. Leung, Y. Liu, and K.-L. Teo, "Transformations for nonideal uniform circular arrays operating in correlated signal environments," *IEEE Trans. On Signal Processing*, vol. 54, no. 1, pp. 34–48, Jan 2006.

[10] B. Lau and Y. Leung, "A dolph-chebyshev approach to the synthesis of array patterns for uniform circular arrays," in *Circuits and Systems, 2000. Proceedings. ISCAS 2000 Geneva. The 2000 IEEE International Symposium on*, vol. 1, 2000, pp. 124–127.

[11] T.-E. Wang, R. Brinkman, and K. Baker, "Dolph-chebyshev pattern synthesis for uniform circular arrays," in *Wireless at VT*, April 2011, pp. 1–9.

[12] W. Dorsey, J. Coleman, R. Kindt, and R. Mital, "Second-order cone programming for scan-plane reconstruction for the wavelength-scaled array," *IEEE Trans. Antennas Propag.*, vol. 62, no. 5, pp. 2826–2831, May 2014.

[13] D. P. Scholnik and J. O. Coleman, "Optimal array-pattern synthesis for wideband digital transmit arrays," *IEEE J. Sel. Topics Signal Process., Special Issue on Convex Optimization Methods for Signal Process.*, vol. 1, no. 4, pp. 660–677, Dec. 2007.

[14] J. O. Coleman, D. P. Scholnik, and P. E. Cahill, "Synthesis of a polarization-controlled pattern for a wideband array by solving a second-order cone program," in *Proc. IEEE Int. Symp. on Antennas and Propag.*, vol. 2B, 2005, pp. 437–440.

[15] J. O. Coleman, "Nonseparable Nth-band filters as overlapping-subarray tapers," in *Proc. IEEE Radar Conf.*, May 2011, pp. 141–146.

[16] K. Tsui and S. Chan, "Pattern synthesis of narrowband conformal arrays using iterative second-order cone programming," *IEEE Trans. Antennas Propag.*, vol. 58, no. 6, pp. 1959–1970, June 2010.

[17] J. Coleman, D. Scholnik, and J. Brandriss, "A specification language for the optimal design of exotic fir filters with second-order cone programs," in *Signals, Systems and Computers, 2002. Conference Record of the Thirty-Sixth Asilomar Conference on*, vol. 1, nov. 2002, pp. 341–345.

[18] H. Lebret and S. Boyd, "Antenna array pattern synthesis via convex optimization," *IEEE Trans. Signal Process.*, vol. 45, no. 3, pp. 526–532, 1997.

[19] M. Lobo, L. Vandenberghe, S. Boyd, and H. Lebret, "Applications of second-order cone programming," *Linear Algebr. Applicat.*, vol. 248, pp. 193–228, Nov. 1998.

[20] J. O. Coleman, "Tapers for large planar phased arrays on regular grids: Simple design methods versus second-order cone programming," in *European Signal Process. Conf.*, Aalborg, Denmark, Aug. 23–27, 2010.

[21] D. P. Scholnik and J. O. Coleman, "Superdirectivity and snr constraints in wideband array-pattern design," in *Proc. IEEE Radar Conf.*, Atlanta GA, USA, May 2001, pp. 181–186.

[22] J. F. Sturm, "Using SeDuMi 1.02, a Matlab toolbox for optimization over symmetric cones," *Optimization methods and software*, vol. 11–12, pp. 625–653 (versions 1.02/1.03), 1999, updated in 2001 for version 1.05. [Online]. Available: http://www.optimization-online.org/DB_HTML/2001/10/395.html

[23] Imre Pólik and Tamás Terlaky. SeDuMi 1.3. Cor@l Lab: Computational Optimization Research at Lehigh. Lab website: http://coral.ie.lehigh.edu/. [Online]. Available: http://sedumi.ie.lehigh.edu/

[24] R. J. Vanderbei and H. Yurttan, "Using LOQO to solve second-order cone programming problems," *Constraints*, vol. 1, 1998. [Online]. Available: http://www.academia.edu/download/30589187/socp.pdf

[25] R. J. Vanderbei, "LOQO: An interior point code for quadratic programming," *Optimization methods and software*, vol. 11, no. 1–4, pp. 451–484, 1999. [Online]. Available: http://dx.doi.org/10.1080/10556789908805759

[26] ——, *LOQO User's Manual—Version 4.05*, Technical Report ORFE-99-(TBD), Dept. of Operations Research and Financial Engineering, Princeton University, Sep. 13, 2006. [Online]. Available: http://www.princeton.edu/~rvdb/tex/loqo/loqo405.pdf

[27] ——. LOQO optimization software. Dept. of Operations Research and Financial Engineering, Princeton University. [Online]. Available: http://www.princeton.edu/~rvdb/loqomenu.html

[28] K.-C. Toh, M. J. Todd, and R. H. Tütüncü, "SDPT3—a Matlab software package for semidefinite programming," *Optimization methods and software*, vol. 11, pp. 545–581, 1999. [Online]. Available: http://www.tandfonline.com/doi/abs/10.1080/10556789908805762

[29] R. H. Tütüncü, K.-C. Toh, and M. J. Todd, "Solving semidefinite-quadratic-linear programs using SDPT3," *Ser. B*, vol. 95, no. 2, pp. 189–217, 2003. [Online]. Available: http://dx.doi.org/10.1007/s10107-002-0347-5

[30] K.-C. Toh, M. J. Todd, and R. H. Tütüncü. (2006, Jul. 17) SDPT3 version 4.0—a MATLAB software for semidefinite-quadratic-linear programming. Dept. of Mathematics, National Univ. of Singapore. [Online]. Available: http://www.math.nus.edu.sg/~mattohkc/sdpt3.html

[31] AMPL Optimization LLC. AMPL®: A modeling language for mathematical programming. [Online]. Available: http://www.ampl.com/

[32] M. Grant and S. Boyd, "Graph implementations for nonsmooth convex programs," in *Recent Advances in Learning and Control*, ser. Lecture Notes in Control and Information Sciences, V. Blondel, S. Boyd, and H. Kimura, Eds. Springer-Verlag, 2008, pp. 95–110. [Online]. Available: http://stanford.edu/~boyd/graph_dcp.html

[33] ——, "CVX: Matlab software for disciplined convex programming, version 2.0 (beta)," Sep. 2012. [Online]. Available: http://cvxr.com/cvx

[34] J. O. Coleman, D. P. Scholnik, and J. J. Brandriss, "A specification language for the optimal design of exotic FIR filters with second-order cone programs," in *Proc. IEEE Asilomar Conf. on Signals, Systems and Computers*, vol. 1, Nov. 2002, pp. 341–345, note: the IEEEXplore version is damaged, so find a preprint.

[35] The Mathworks. MATLAB®: A a high-level language and interactive environment for numerical computation, visualization, and programming. [Online]. Available: http://www.mathworks.com/

[36] J. Coleman, K. McPhail, P. Cahill, and D. Scholnik, "Efficient subarray realization through latering," in *Antenna Applications Symp.*, Monticello IL, USA, Sep. 21–23, 2005. [Online]. Available: http://www.dtic.mil/docs/citations/ADM001873

[37] D. Kelley and W. Stutzman, "Array antenna pattern modeling methods that include mutual coupling effects," *IEEE Trans. Antennas Propag.*, vol. 41, no. 12, pp. 1625–1632, 1993.

[38] J. Coleman and D. Scholnik, "Design of nonlinear-phase fir filters with second-order cone programming," in *Proc. 1999 Midwest Symp. on Circuits and Systems*, vol. 1, 1999, pp. 409–412.